

Analysis and Design of Position-Force Teleoperation with Scattering Matrix ^{*}

Minh Duc Duong^{*} Takanori Miyoshi^{*} Kazuhiko Terashima^{*}
Erick J. Rodriguez-Seda^{**}

^{*} Toyohashi University of Technology, Toyohashi, Aichi, Japan,
(e-mail: duc,miyoshi,terasima@syscon.pse.tut.ac.jp).

^{**} University of Illinois at Urbana-Champaign, Urbana, IL 61801, USA
(e-mail: erodrig4@uiuc.edu)

Abstract: This paper presents a design method for a position-force bilateral teleoperation system with scattering matrix by using compensators and wave filters. At first, the compensators and low-pass filters were chosen to guarantee the system's stability based on the small-gain theorem. After that, the effects of wave impedance and time delay on the stiffness and the viscosity of the system were evaluated. Moreover, the existence of oscillation, and even instability of the local loop caused by properties of remote environment, are recognized and explained. Finally, the conditions for the designed parameters to stabilize the system are given using Popov criterion.

1. INTRODUCTION

Teleoperation, where a human operator conducts a task in a remote environment via master and slave manipulators, has a wide field of applications such as telemanufacturing, telemaintenance, telesurgery, rescue and so on. Bilateral teleoperation, in which contact force information is provided directly to the human operator, can improve task performance. However, when teleoperation is performed via a time delay communication environment, this delay can destabilize a bilaterally controlled teleoperator.

The instability problem of bilateral operation systems survived until 1989, when Anderson and Spong [1989] used passivity and the scattering theory to overcome this problem for arbitrary constant time delay. In addition, Niemeyer and Slotine [1991] clarified the scattering matrix from the standpoint of the energy balance. Although velocity-force architecture teleoperation systems could be stabilized based on the above researches, it has remained difficult to improve both the stability and transparency for teleoperation systems with time delay. The reason for this difficulty is that position-force architecture cannot be used, because of its non-passive property. Moreover, as long as the passivity concept is used, the human operator and the remote environment must be passive.

In order to overcome the non-passive problem of position-force architecture when using the scattering matrix, Miyoshi, et. al [2006] proposed a design method utilizing wave filters to stabilize a non-passive operating system. In this method, the scattering matrix is used, but it is considered with regard to its frequency characteristics rather than passivity concepts. Therefore, the position-force architecture can be adopted, and passivity of the operator and environment is not required. However, the

effects of wave impedance, have not been carefully evaluated. Moreover, the local loop created by the scattering matrix at each local site has not yet been considered. That local loop contains the environment and may destabilize the system.

In the present study, we at first analyzed the effects of the scattering matrix on the position-force architecture teleoperation system in Miyoshi, et. al [2006] by considering the frequency characteristics of the scattering matrix and the local loop created by the scattering matrix. In this system, the relation of the designed parameters has been clarified to guarantee the stability of the system. In addition, the stiffness and viscosity of the system are calculated to evaluate the effects of wave impedance and time delay on the feeling of the human operator. Moreover, the system has nonlinear properties, such as the environment force is zero when the robot moves freely, and non-zero when the robot makes contact with the environment. The present nonlinear response of the remote environment may cause oscillation or even instability of the local loop created by the scattering matrix. This research allows us to identify the conditions that stabilize the local loop, thereby stabilizing the whole system.

The paper is organized as follows: the frequency characteristics of the scattering matrix, and the design method based on the small gain theorem of H_∞ norm are given in Section II. In Section III, the effects of wave impedance and time delay on the system's performance are presented. The problems of the local loop created by the scattering matrix are shown in Section IV. To conclude, Section V provides a discussion of the results and some remarks.

^{*} This work was supported by Global COE Program "Frontiers of Intelligent Sensing" from the Ministry of Education, Culture, Sports, Science and Technology, Japan.

2. TELEOPERATION SYSTEM WITH THE SCATTERING MATRIX

2.1 Model of the teleoperation system with the scattering matrix

A fundamental block diagram of the bilateral teleoperation system with the scattering matrix is shown in Fig. 1. The human applies his force $f_h(t)$ to the master robot; the master robot also receives feedback force $f_m(t)$ from the slave site. The input force moves the master robot, and the movement information, $y_m(t)$, is sent to the slave site. At the slave site, the slave robot is moved according to the movement information $y_r(t)$. The contact force of the slave robot to the environment $f_s(t)$ is also transmitted back to the master site. The transfer functions $W_m(s)$ and $W_s(s)$ in Fig. 1 are filters and will be explained later. T_1 and T_2 are the constant time delays, and b is a positive constant (matrix) known as the wave impedance. $G_m(s)$ and $G_s(s)$ are transfer functions of the master and the slave robot respectively.

$$G_m(s) = \frac{Y_m(s)}{-F_m(s)}, G_s(s) = \frac{F_s(s)}{Y_r(s)}. \quad (1)$$

The wave variables u_m, v_m, u_s, v_s given by.

$$\begin{aligned} u_m &= \frac{1}{\sqrt{2b}}(f_m + by_m), v_m = \frac{1}{\sqrt{2b}}(f_m - by_m), \\ u_s &= \frac{1}{\sqrt{2b}}(f_s + by_r), v_s = \frac{1}{\sqrt{2b}}(f_s - by_r). \end{aligned} \quad (2)$$

while G_{mm} and G_{ss} are defined as follows:

$$G_{mm}(s) = U_m(s)/V_m(s), G_{ss}(s) = V_s(s)/U_s(s). \quad (3)$$

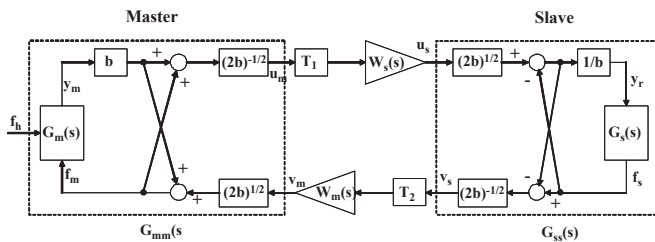


Fig. 1. The bilateral teleoperation system with the scattering matrix

2.2 Stability of the velocity-force architecture teleoperation

Under velocity-force architecture in Anderson and Spong [1989], movement information is velocity, and the contact force that is transmitted back to the master site is the coordinating force (the output of the PI controller of the slave robot). In addition, under the assumption that the human operator and the environment are passive, then G_m and G_s are passive.

From (2) and (3), G_{ss} can be calculated as

$$G_{ss}(s) = \frac{G_s(s) - b}{G_s(s) + b} \quad (4)$$

Then

$$\begin{aligned} |G_{ss}(j\omega)|^2 &= G_{ss}(j\omega)G_{ss}(-j\omega) \\ &= \frac{(Re\{G_s(j\omega)\} - b)^2 + Im\{G_s(j\omega)\}^2}{(Re\{G_s(j\omega)\} + b)^2 + Im\{G_s(j\omega)\}^2}, \end{aligned} \quad (5)$$

where $Re\{G_s(j\omega)\}$ and $Im\{G_s(j\omega)\}$ are real and image parts of $G_s(j\omega)$, respectively.

Because G_s is passive, $Re\{G_s(\omega)\} \geq 0$ (Slotine and Li [1991]). Therefore

$$|G_{ss}(j\omega)|^2 = \frac{(Re\{G_s(\omega)\} - b)^2 + Im\{G_s(\omega)\}^2}{(Re\{G_s(\omega)\} + b)^2 + Im\{G_s(\omega)\}^2} \leq 1$$

This leads to $\|G_{ss}(s)\|_\infty \leq 1$.

Similarly, we can get $\|G_{mm}(s)\|_\infty \leq 1$.

By choosing $W_m(s) = W_s(s) = 1$, we have

$$J_\infty = \|G_{mm}(s)W_m(s)\|_\infty \|G_{ss}(s)W_s(s)\|_\infty \leq 1 \quad (6)$$

With invariant time delay, following the small gain theorem, the system is stable.

2.3 Teleoperation system with position-force architecture

Under position-force architecture, the movement information is position, and the contact force that is transmitted back to the master site is the measured force. Therefore, the system is no longer passive and the problem is to design the wave filters $W_m(s)$ and $W_s(s)$ such that (6) is satisfied.

A. System model Fig. 2 shows the block diagram of the master site.

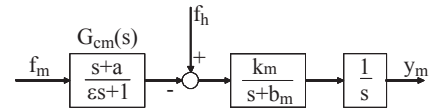


Fig. 2. Master site's model

Here, the master robot model is assumed to be

$$P_m(s) = \frac{Y_m(s)}{F_h(s) - F_r(s)} = \frac{k_m}{s(s + b_m)}, \quad (7)$$

where

$$F_r(s) = G_{cm}F_m(s) = \frac{s + a}{\epsilon s + 1}F_m(s). \quad (8)$$

The purpose of introducing G_{cm} will be explained later.

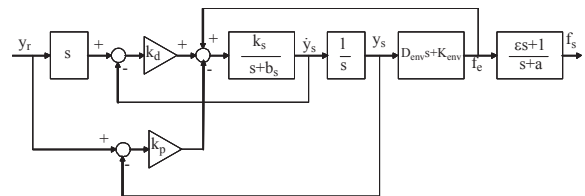


Fig. 3. Slave site's model

Fig. 3 shows the block diagram of the slave site. The slave robot model is assumed to be

$$\frac{Y_s(s)}{V_s(s)} = \frac{k_s}{s(s + b_s)}, \quad (9)$$

where $Y_s(t)$ is the slave robot position and $V_s(t)$ is the motor voltage.

The slave robot is controlled by a Proportional-Derivative (PD) Controller.

$$V_s(t) = k_p(y_r(t) - y_s(t)) + k_d(\dot{y}_r(t) - \dot{y}_s(t)) \quad (10)$$

We assume that the environment is a spring-damper type. The environmental force $f_e(t)$ is caused by the spring stiffness $K_{env} \times y_s(t)$ and damping $D_{env} \times \dot{y}_s(t)$. As such,

$$F_e(s) = (D_{env}s + K_{env})Y_s(s) \quad (11)$$

The feedback force $F_s(s)$ is related to the environmental force $F_e(s)$ by

$$F_s(s) = G_{cs}(s)F_e(s) = \frac{\epsilon s + 1}{s + a} F_e(s) \quad (12)$$

The purpose of introducing G_{cs} is also explained later.

Finally, we have the transfer function of the slave site as

$$G_s(s) = G_{cs}(s) \frac{F_e(s)}{X_r(s)} = \frac{\epsilon s + 1}{s + a} \frac{k_s(k_d s + k_p)(D_{env}s + K_{env})}{s^2 + (b_s + k_s(k_d + D_{env}))s + k_s(k_p + K_{env})} \quad (13)$$

B. Choosing of compensators and wave filters The purpose of the compensators and wave filters is to satisfy (6), i. e, to guarantee the stability of the system with invariant time delay. In the master site, in order to get $\|G_{mm}(s)\|_\infty \leq 1$ or as small as possible, instead of using the wave filter $W_m(s)$ such as in the slave site, a phase-lead compensator $G_{cm}(s) = (s + a)/(\epsilon s + 1) \sim s + a(0 < a < b_m, \epsilon \ll 1)$ is used as the design of the wave filter may require some conditions that are difficult for the master site.

In contrast, by using G_{cm} in the master site, the phase-lag compensator $G_{cs}(s) = 1/G_{cm}(s)$ must be used in the slave site to maintain the physical relationship between environmental force $f_e(t)$ and implemented feedback force at the master site $f_r(t)$. Although G_{cs} makes the slave site non-passive and $|G_{ss}(j\omega)| > 1$, its frequency range is relatively high. Therefore, we can get $J_\infty \leq 1$ by an adequate low-pass filter $W_s(s)$.

The low-pass filter $W_s(s)$ should be chosen so that $\|G_{ss}(s)W_s(s)\|_\infty \leq 1$, and therefore, the inequality (6) is satisfied.

From (5), it is found that

$$\begin{aligned} |G_{ss}(j\omega)| &\leq 1 \text{ if } \operatorname{Re}\{G_s(j\omega)\} \geq 0 \\ |G_{ss}(j\omega)| &> 1 \text{ if } \operatorname{Re}\{G_s(j\omega)\} < 0 \end{aligned}$$

Fig. 4 describes this characteristic of the scattering matrix. Therefore, $W_s(s)$ is chosen such that $|W_s(j\omega)| = 1$ at frequencies such that $\operatorname{Re}\{G_s(j\omega)\} > 0$, and $|W_s(j\omega)| \ll 1$ at frequencies such that $\operatorname{Re}\{G_s(j\omega)\} \leq 0$. This choice makes $\|G_{ss}(s)W_s(s)\|_\infty \leq 1$ and (6) is satisfied.

Commonly, there exists a frequency ω_0 such that

$$\begin{aligned} \operatorname{Re}\{G_s(j\omega)\} &> 0 \text{ if } \omega < \omega_0 \\ \operatorname{Re}\{G_s(j\omega)\} &= 0 \text{ if } \omega = \omega_0 \\ \operatorname{Re}\{G_s(j\omega)\} &< 0 \text{ if } \omega > \omega_0 \end{aligned}$$

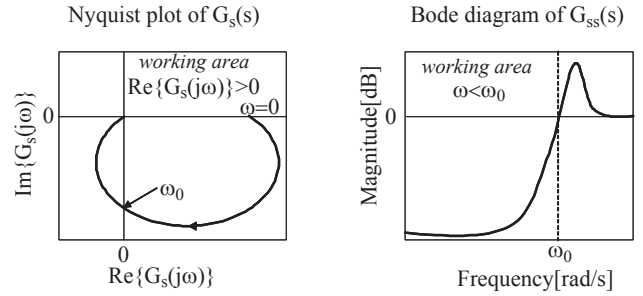


Fig. 4. The Nyquist plot of $G_s(s)$ (left figure) and the Bode diagram of G_{ss} (right figure).

The filter $W_s(s)$ is a low-pass filter with cut-off frequency ω_0 that is determined from $G_s(s)$.

However, depending on the application of the teleoperation system, the working frequency range is required (for example, the frequency range is from 0 Hz to 5 Hz). The cut-off frequency ω_0 usually has the lower limit, $\omega_0 \geq \omega_{min}$. Therefore, adjustable parameters of $G_s(s)$ such as the parameters k_p, k_d of the PD controller should be determined carefully, in order that the corresponding ω_0 satisfies the lower bound condition. To do that, instead of deriving ω_0 from equation $G_s(\omega_0) = 0$, which might be complicated, the condition of k_p, k_d is derived from inequality $\operatorname{Re}\{G_s(j\omega_{min})\} \geq 0$.

C. Experimental Results The experiment was carried out with the same master-slave robot system as in Rodríguez-Seda, et. al [2006]. This system has two degree of freedom (DOF). However, for linearity and simplicity, we only work with a 1DOF robot system, and the other joint is fixed. The remote environment is a wall for which the stiffness can be changed. The parameters for the experiment are shown in Table I. Note that when we design the wave filter,

Table 1. Typical parameters of experiments

Parameter	Unit	Value
D_{env}	[N/(rad/s)]	0
K_{env}	[N/rad]	0-1000
k_p	-	300
k_d	-	30
T_1	[s]	0.1
T_2	[s]	0.1
a	-	2
ϵ	-	0.01
b	-	20
$W_m(s)$	-	1
$W_s(s)$	-	$\frac{1}{(0.03s+1)^2}$

K_{env} is considered in the range mentioned in Table I, but in the experiment, K_{env} is a constant value.

The experimental results are as shown in Fig. 5 and Fig. 6 for position and force data, respectively. From these figures, it can be seen that the system almost has good position and force tracking. At the time the slave robot touches the wall, there is a difference between the positions of the master and the slave robots. However, this difference will be compensated for. When the slave robot stops, the environmental force becomes constant. After a period of time equaling the time delay, the system updates the information, and the forces at both sites are balanced thus

compensating for the position difference. When the slave robot is in free movement, there is also a difference between environmental force and feedback force. This difference is caused by the viscosity of the system that is discussed in the next section.

Regarding the feeling of the human operator, when he moves the master arm freely, he feels the viscosity of the system. And when the time delay increases, he must use more force to move the robot. The same situation occurs when the wave impedance is increased. This relation is explained clearly in the next sections.

When we increase the stiffness of the environment, the system may become oscillatory or even unstable. This instability is caused by the local loop created by the scattering matrix at the slave site, and we will consider this situation in the next sections.

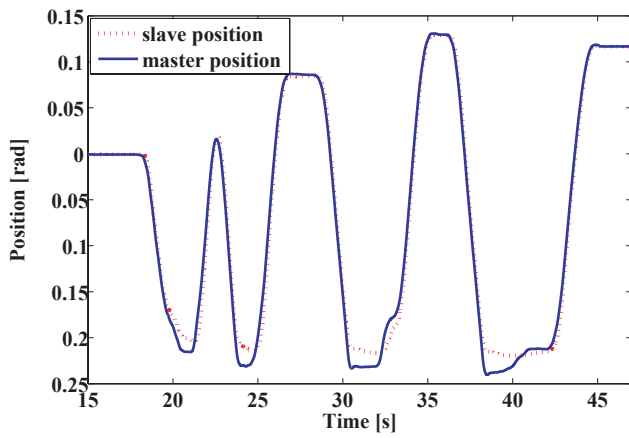


Fig. 5. Experimental result of the master and the slave robot position

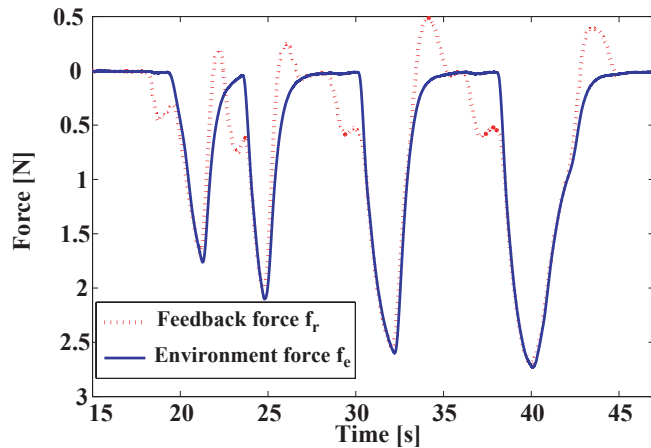


Fig. 6. Experimental result of environment force and feedback force

3. PERFORMANCE OF THE POSITION-FORCE TELEOPERATION SYSTEM

It is easily found that by using the scattering matrix, at a steady state, $y_r = y_m$ and $f_m = f_s$. Therefore, good position tracking can be obtained by the PD controller

at the slave site. However, since the human operates the system by moving the master arm, the feeling stiffness and viscosity of the system are also very important. In this section, the stiffness of the system during contact with the remote environment and the viscosity of the system during free movement (non-contact) are respectively evaluated considering the wave impedance and communication time delay.

From (3), (4), (8), and (13), we can derive the relation

$$\begin{aligned} F_m(s) &= -b \frac{V_m(s)/U_m(s) + 1}{V_m(s)/U_m(s) - 1} Y_m(s) \\ &= -b \frac{H_s(s) + 1}{H_s(s) - 1} Y_m(s), \end{aligned} \quad (14)$$

where

$$H_s(s) = e^{-sT} W_m(s) W_s(s) G_{ss}(s),$$

with $T = T_1 + T_2$ being the round trip delay (RTT).

Then,

$$\frac{Y_m(s)}{F_h(s)} = \frac{1 - H_s(s)}{\frac{1 - H_s(s)}{P_m(s)G_{cm}(s)} + b(1 + H_s(s))} \frac{1}{G_{cm}(s)}, \quad (15)$$

$$\frac{\dot{Y}_m(s)}{F_h(s)} = \frac{(1 - H_s(s))P_m(s)s}{(1 - H_s(s) + b(1 + H_s(s))P_m(s)G_{cm}(s))} \quad (16)$$

In the case of contact with the remote environment, the stiffness at the steady state can be calculated from (15), and the result is

$$\left. \frac{Y_m(s)}{F_h(s)} \right|_{s=0} = \frac{k_p + K_{env}}{k_p K_{env}} = \left. \frac{Y_r(s)}{F_s(s)} \right|_{s=0}$$

Accordingly, the stiffness $F_h(s)/Y_m(s)$ in the steady state at the master site is consistent with the stiffness of the slave site, which includes the environment and the position controller, regardless of time delay.

In the case of free motion (non-contact, $G_s(s) = 0$), then $H_s(s) = -e^{-sT} W_m(s) W_s(s)$. In order to simplify, suppose that the low-pass filter $W_s(s)$ is equivalent to a first-order low-pass filter of $W_s(s) = 1/(T_s s + 1)$, ($W_m(s) = 1$). The viscosity of the system that the human operator feels at the steady state can be calculated from (16), and the result is as follows

$$\left. \frac{F_h(s)}{Y_m(s)} \right|_{s=0} = \frac{b_m}{k_m} + \frac{ab}{2}(T + T_{s0})$$

The viscosity is the sum of the viscosity of the master robot itself and a part that is proportional to wave impedance b and round trip delay T . Therefore, there is a difference between the feedback force f_r and environmental force f_e . Moreover, the human feels higher viscosity if the time delay or the wave impedance b is increased.

4. LOCAL LOOP CREATED BY THE SCATTERING MATRIX

The scattering matrix creates a local loop at both the master site and the slave site. It is easily found that the local loop in the master site is stable. However, the local loop in the slave site that includes the remote environment

may cause instability in the slave site. In this section, we evaluate the stability of the local loop in the slave site shown in Fig. 7.

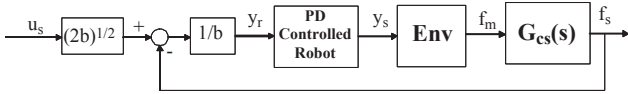


Fig. 7. Local loop created by the scattering matrix at the slave site

4.1 Condition of absolute stability at the slave site

Let us consider the case that the slave robot collides with a wall. Before the collision, the measured force is zero. At the position x_0 , the robot touches the wall and the wall resists the robot's movement. Therefore, the response of the environment (in this case, the wall) is as follows:

Suppose that $x_0 = 0$,

$$f_e = \phi(x) = \begin{cases} 0 & \text{if } x \leq 0 \\ K_{env}x & \text{if } x > 0 \end{cases} \quad (17)$$

Here, we consider the environment with high stiffness, with the damping factor being much smaller than the stiffness, and the damping factor is therefore ignored. Fig. 8 shows the response of the environment corresponding to the slave robot position.

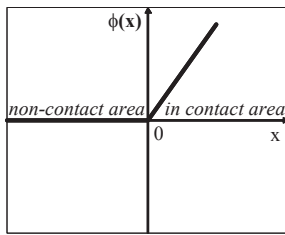


Fig. 8. The environment force versus slave robot position

The non-linear characteristics of the environment may cause oscillation or even the system instability. In order to stabilize the local loop in the slave site, we derive the condition for absolute stability using the Popov criterion (Khalil [1996]). Fig. 9 shows the block diagram of the local loop for the purpose of using the Popov criterion.

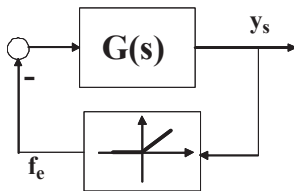


Fig. 9. Diagram of the local loop at the slave site for using Popov criterion

The transfer function $G(s)$ of the open loop is

$$G(s) = G_1(s) + G_2(s), \quad (18)$$

$$G_1(s) = \frac{k_s}{s^2 + (b_s + k_s k_d)s + k_s k_p}, \quad (19)$$

$$G_2(s) = \frac{k_s}{b} \frac{(\epsilon s + 1)(k_d s + k_p)}{(s + a)(s^2 + (b_s + k_s k_d)s + k_s k_p)} \quad (20)$$

Because $\epsilon \ll 1$,

$$G_2(s) = \frac{k_s}{b} \frac{k_d s + k_p}{(s + a)(s^2 + (b_s + k_s k_d)s + k_s k_p)} \quad (21)$$

The nonlinear function $\phi(x)$ satisfies the condition

$$\phi(x)(\phi(x) - Kx) \leq 0, \forall x \quad (22)$$

with $K \geq K_{env}$. Because K_{env} can be any value, K should be chosen to be infinite, $K = +\infty$

The Popov criterion said that if there exist $\eta \geq 0$ such that the Popov plot ($Re\{G(j\omega)\}$ versus $\omega Im\{G(j\omega)\}$) lies to the right of the line that intercepts the point $-1/K + j0$ with the slope $1/\eta$, the system is absolute stable.

In our case, $K = +\infty$, and the shape of the Popov plot is as shown in Fig. 10(a). Therefore, the condition to ensure the absolute stability of the system in Fig. 7 is $\omega Im\{G(j\omega)\} \leq 0$.

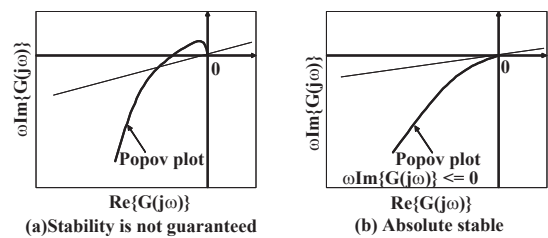


Fig. 10. Popov plot in two cases: (a) the stability is not guaranteed and (b) absolute stable

We have $G(j\omega) = G_1(j\omega) + G_2(j\omega)$, and after some simple calculations from (19), we can obtain $\omega Im\{G_1(j\omega)\} < 0$. Therefore, the condition for absolute stability now is $\omega Im\{G_2(j\omega)\} \leq 0$.

From (21), after some calculations, we get the condition $\omega Im\{G_2(j\omega)\} \leq 0$ is equivalent to

$$k_d(a + b_s + k_s k_d) \geq k_p \quad (23)$$

This is also the condition for the absolute stability of the system in Fig. 7

4.2 Stable validation of the slave site

The validation is carried out by simulation under the condition with the initial position of $1[rad]$, the initial velocity of $1[rad/s]$, $k_s = 1.3$, $b_s = 0.65$, $\epsilon = 0.001$, $a = 1$, $K_{env} = 100$ and $b = 1$. Fig. 11 shows the Popov plot and the phase portrait of the system with $k_p = 100$, $k_d = 0.83$. It is clear that the inequality (23) is not satisfied, the Popov criterion is also not satisfied, and the phase portrait of the system converges to a limit-cycle. The system is oscillated.

In the case of $k_p = 100$, $k_d = 10$, the inequality (23) is satisfied. As shown in Fig. 12, the Popov criterion is also satisfied, and the phase portrait of the system converges to the origin.

4.3 Problems to practice

The Popov criterion guarantees the absolute stability of the system; however, it does not guarantee fast convergence to the equilibrium point. In some cases, the system oscillates before converging to an equilibrium point. This

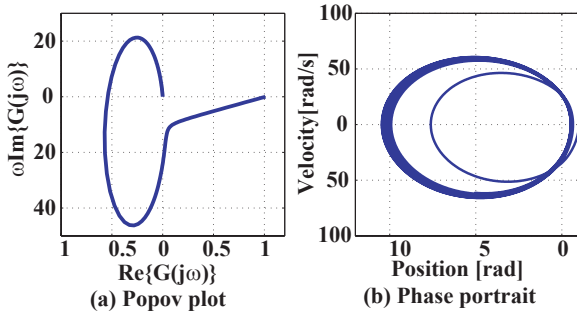


Fig. 11. The Popov plot and the phase portrait with $k_p = 100$, $k_d = 0.83$

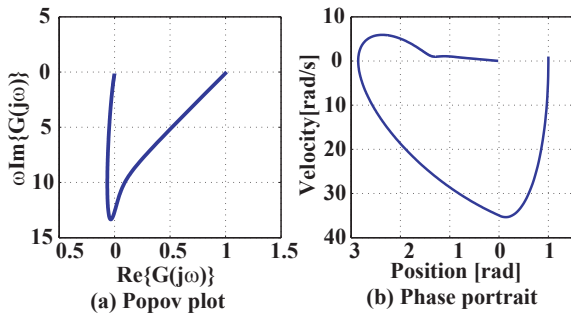


Fig. 12. The Popov plot and the phase portrait with $k_p = 100$, $k_d = 10$

phenomenon should be avoided in the practice. Therefore, a control system guaranteeing only absolute stability is not enough in practice. This problem will be considered in future study.

5. CONCLUSION

Bilateral teleoperation system of the position-force architecture using the scattering matrix can be stabilized by using compensators and wave filters, despite its non-passive property. Good tracking with regard to both position and contact force can be achieved.

The working frequency range of the system depends on the application's requirements. The wave filters must maintain this frequency range, and therefore the designed parameters of the controller (k_p and k_d) must be chosen to match the bandwidth of the filter. Moreover, in order to stabilize the local loop created by the scattering matrix, the designed parameters must satisfy some conditions. At the steady state, when the robot moves freely, the human operator feels the viscosity that is proportional to the wave impedance b . Therefore b should be a small value. The viscosity is also proportional to the round trip time delay T , and it is harder to work with the larger time delay. If the robot is in contact with the environment, transparency is obtained.

This design method can guarantee system stability. However, in practice, the oscillation may occur before the system converges to the stable steady state. This phenomenon is undesired and the future study will require obtaining fast convergence for the system.

ACKNOWLEDGEMENTS

The authors would like to thank Prof. Mark W. Spong at the Coordinated Science Laboratory, University of Illinois (UIUC) for his permission and support to carry out the experiment in the master-slave robot system at his laboratory.

REFERENCES

- R. J. Anderson and M. W. Spong. Bilateral Control of Teleoperators with Time Delay. *IEEE Trans. on Automatic Control*, Vol. 34, No. 5, pages 494–501, May, 1989.
- G. Niemeyer and J. J. E. Slotine Stable Adaptive Teleoperation. *IEEE Journal of Oceanic Engineering*, Vol. 16, No. 1, pages 152–162, January, 1991.
- T. Miyoshi, K. Terashima, and M. Buss. A Design Method of Wave Filter for Stabilizing Non-Passive Operation System. *Proceedings of 2006 IEEE Int. Conf. on Control Applications*, pages 1318–1324, October, 2006.
- Erick J. Rodriguez-Seda, Dongjun Lee and Mark W. Spong. An Experimental Comparison Study for Bilateral Internet-Based Teleoperation. *Proceedings of 2006 IEEE Int. Conf. on Control Applications*, pages 1701–1706, October, 2006.
- Khalil, Hassan K. *Nonlinear Systems*, Second Edition, Prentice-Hall, pages 419–423, 1996.
- Jean-Jacques E. Slotine and Weiping Li. *Applied Nonlinear Control*, Prentice-Hall, pages 132-142, 1991